Cranial bone histology of *Metoposaurus krasiejowensis* (Amphibia, Temnospondyli) from the Late Triassic of Poland

Kamil Gruntmejer Corresp., [1, 2] , **Dorota Konietzko-Meier** [1, 2, 3] , **Adam Bodzioch** [1]

[1] Department of Biosystematics, University of Opole, Opole, Poland
[2] European Centre of Palaeontology, University of Opole, Opole, Poland
[3] Steinmann Institute, University of Bonn, Bonn, Germany

Corresponding Author: Kamil Gruntmejer
Email address: gruntmejerkamil@gmail.com

In this study a detailed description of the 21 skull bones of *Metoposaurus krasiejowensis* from the Late Triassic of Poland is presented. All dermal bones show a diploë structure, with the ornamented external surface. The ridges consist of well vascularized parallel-fibered bone; the valleys are built of an avascular layer of lamellar bone. The dense clumps of thin, well mineralized Sharpey's fibers are preserved. The growth marks are manifested in four ways: a sequence of resting lines; layers of lamellar bone alternated with layers with Interwoven Structural Fibers (ISF); thick, avascular annuli and high vascularized zones; and the alternations of valleys and ridges. The thick middle region consists of cancellous bone, with varying porosity. The thin and less vascularized internal cortex consists of parallel-fibered bone. Calcified cartilage is observed in the quadrate and the exoccipital. The skull bones show strong variability within the microanatomical and histological levels. The histological framework is not bone-limited, but varies even in one single bone; this seems to be related to the specific position of the bone and depends on the local biomechanical loading of the particular part of the skull. The large accumulation of Sharpey's fibers in the occipital condyles indicates the presence of strong muscles and ligaments connecting the skull to the vertebral column. The dynamic processes during the ornamentation deposition are observed indicate that the position of the ridges and grooves change during the growth and could be the specific adaptation to biomechanical conditions and stress distribution during the bone development. In the supratemporal the cementing lines indicated the remodeling process could be involved into the creations of sculpture.

Cranial bone histology of *Metoposaurus krasiejowensis* (Amphibia, Temnospondyli) from the Late Triassic of Poland

Kamil Gruntmejer[1,2,*], Dorota Konietzko-Meier[1,2,3], Adam Bodzioch[1]

[1] Opole University, Department of Biosystematics, Laboratory of Palaeobiology, Oleska 22, 45-052 Opole, Poland

[2] Opole University, European Centre of Palaeontology, Oleska 48, 45-052 Opole, Poland

[3] University of Bonn, Steinmann Institute, Nussallee 8, 53115 Bonn, Germany

*gruntmejerkamil@gmail.com

* - corresponding author

ABSTRACT

In this study a detailed description of the 21 skull bones of *Metoposaurus krasiejowensis* from the Late Triassic of Poland is presented. All dermal bones show a diploë structure, with the ornamented external surface. These bones show strong variability within the microanatomical and histological levels. The external cortex of ridges consist of parallel-fibered bone, mostly well vascularized; the valleys are built of an avascular layer of lamellar bone. The dense clumps of thin, well mineralized Sharpey's fibers are there preserved. The thick middle region consists of cancellous bone, with varying porosity. The thin and less vascularized internal cortex consists of parallel-fibered bone. The cyclity of growth is manifested as an alternation of thick, avascular annuli and high vascularized zones as well as a sequence of resting lines. Calcified cartilage is observed in the quadrate and the exoccipital. The histological framework varies even within one bone; this seems to be related to the specific area and depends on the local biomechanical loading of the particular part of the skull. The large accumulation of Sharpey's fibers in the occipital condyles indicates the presence of strong muscles and ligaments connecting the skull to the vertebral column. The dynamic processes observed during the ornamentation creation indicate that the position of the ridges and grooves change during growth and could be the specific adaptation to changing biomechanical conditions and stress distribution during the bone development. In the supratemporal the cementing lines show that the remodeling process could be involved into the creations of sculpture.

Keywords:
Temnospondyli, dermal bones, skull, histology, microanatomy

INTRODUCTION

Metoposaurids were large, up to 3 meters long, late Triassic Temnospondyli with a strongly dorso-ventrally flattened body, and adapted to aquatic life. The most characteristic and best known part of the *Metoposaurus* skeleton is the extremely flat parabolic skull with anteriorly located orbits (e.g. Schoch & Milner, 2000). The temnospondyl skull functionally represents one skeletal element, however, anatomically, it is a conglomerate of numerous bones various in shape and thickness, having various functions and biomechanical loading (i.e. Fortuny et al., 2011, Fortuny et al., 2012).

The flat bones of the skull represent the dermal bones which develop via direct transformation of preexisting connective tissue (Francillon-Vieillot et al., 1990). The external surface of the dermal bones is characteristically ornamented. A network of raised, reticulate ridges that enclose approximately flat-bottomed, interlocking, polygonal cells is the most common type. The vast majority of these cells are four-, five-, or six-sided, creating a honeycomb- or waffle iron-like texture. In some temnospondyls, this is essentially the only texture present. The second texture type comprises raised, parallel to sub-parallel ridges separated by round-bottomed grooves (Rinehart & Lucas, 2013). The function of the ornamentation is still unclear. The best supported hypotheses suggest the increase the surface area for skin supports, increasing the strength of the bone, the protection of blood vessels or a

contribution of bone ornamentation in thermal exchanges (summarized in Coldiron, 1974; Witzmann, 2009; Rinehart & Lucas, 2013; Clarac et al. 2015, 2016).

The histology of the amniotes osteoderms is well known and studied for several groups (e.g. Scheyer & Sander, 2004; Vickaryous & Sire, 2009; Buffrénil et al., 2011; Burns et al., 2013; Scheyer et al., 2014; Cerda et al., 2015 and further references in all). The histology of temnospondyl dermal bones is less known and was first described by Gross (1934), who provided a short description of the skull bones of *Mastodonsaurus*, *Metoposaurus* and *Plagiosternum*, and recognized that the dermal bones exhibit a diploë structure. Later, histological studies on the dermal bones in Temnospondyli have focused mainly on morphology, vascular network and collagen fibers organization (Bystrow, 1947; Enlow & Brown, 1956; Coldiron, 1974; de Ricqlès, 1981; Castanet *et al*, 2003; Scheyer, 2007) and were limited only to the few taxa. The systematic studies of dermal bones within numerous tetrapod taxa were provided by Witzmann (2009) and de Buffrénil et al. (2016). Up until now the dermal bones of *Metoposaurus* have not been studied in detail histologically. The only record of the histological description of *Metoposaurus diagnosticus* dermal bone was given by Gross (1934) and later re-described by Witzmann (2009). However, it is unclear if the illustrated section was derived from the skull or the pectoral girdle, or even if the tested bone-fragment belongs to *Metoposaurus* at all.

The main goal of this study is to present the detailed description of the histology of dermal and endochondral bones from one *Metoposaurus krasiejowensis* (Sulej, 2002) skull and determine, if possible, the tendencies and variability of the histological framework. Moreover, the value of the dermal bones for the skeletonchronological analyses, the ossification modes of the skull and origin of the sculpture will be evaluated.

MATERIAL AND METHODS

Material. The skull (UOPB 01029; 40 cm in length) of *Metoposaurus krasiejowensis* was studied histologically (Figs. 1 and 2). The roof side of the skull was almost completely preserved, whereas on the palatal side only the fragments of the vomer, parasphenoid, pterygoids, quadrates and exoccipitals were preserved. The species discovered in Poland was originally described as *Metoposaurus diagnosticus krasiejowensis* Sulej, 2002, the subspecies of an older *Metoposaurus diagnosticus* (Meyer, 1842). Brusatte *et al*. (2015) resigned using the subspecies for the German *M. diagnosticus diagnosticus* (von Meyer, 1842) and the Polish *M. diagnosticus krasiejowensis* and suggested to refer both taxa on the separate species level as *M. diagnosticus* and *M. krasiejowensis* instead. This taxonomy is followed in this study.

Locality. The examined material comes from the famous locality in Krasiejów where a large number of disarticulated skeletons have been discovered in the Upper Triassic (Keuper), fine-grained, continental sediments. The bones can be found in two main bone-bearing horizons referred to as the lower and the upper horizon (Dzik & Sulej, 2007). The lower horizon has been deposited on an alluvial plain during a catastrophic mud-flow event (Bodzioch & Kowal-Linka, 2012). The skull presented here, has been excavated from the less than 1 m thick lower bone-bearing layer, which is very rich in *Metoposaurus krasiejowensis* remains accompanied by relatively a high diversified fossil assemblage. Vertebrates are represented by a second temnospondyl, *Cyclotosaurus intermedius* Sulej & Majer, 2005, a phytosaur (*Palaeorhinus*; see Dzik, 2001), a typical terrestrial tetrapod aetosaur *Stagonolepis olenkae* Sulej, 2010, pterosaurs (Dzik & Sulej, 2007), sphenodonts and other small tetrapods (Dzik & Sulej, 2007), as well as

fishes (dipnoans described recently by Skrzycki, 2015, and various actinopterygian and chondrichthyan species). Invertebrates, such as unionid bivalves (Dzik et al., 2000; Skawina & Dzik, 2011; Skawina, 2013), cycloids (Dzik, 2008), spinicaudatan crustaceans (Olempska, 2004), fresh-water ostracods (Olempska, 2004, 2011) and some gastropods, are also very common. The upper horizon is restricted to lenses cemented with calcium carbonate, interpreted as a meander deposit (e.g. Gruszka and Zieliński, 2009). It is dominated by strictly terrestrial animals including *Stagonolepis* and the primitive dinosauromorph *Silesaurus opolensis* Dzik, 2003. Aquatic vertebrates such as amphibians and phytosaurs are less common compared to the lower horizon. Apart from that, one fragmentary specimen of the rauisuchian *Polonosuchus silesiacus* (Brusatte et al., 2010) was excavated between the upper and lower horizons.

According to complex stratigraphic studies of the Upper Silesian Keuper, the bone-bearing beds have been deposited in the early Norian times (Racki & Szulc, 2014; Szulc et al., 2015a, b), however, biochronological data uphold the Late Carnian age (e.g. Dzik & Sulej 2007; Lucas et al. 2007; Lucas, 2015).

Methods. The skull was sectioned in 20 planes (Fig. 2) and the thin sections were prepared according to standard petrographic procedures (Chinsamy and Raath, 1992) in the Laboratory of the University of Poznan and in the laboratory of Steinmann Institute (University of Bonn). The thin sections were ground and polished to a thickness of about 60-80 µm using wet SiC grinding powders (SiC 600, 800). Subsequently, the thin sections were studied under a LEICA DMLP light microscope in plane and cross polarized light.

The histological nomenclature follows, with an exception for annuli, Francillon-Vieillot et al. (1990) and Witzmann (2009). According to Francillon-Vieillot et al. (1990) the annual growth cycle consists of a thick, fast growing zone, a thin, slow growing annulus, and a Line of

Arrested Growth (LAG). In this study, the term zone is used as in its traditional meaning, for the highly vascularized layer, with lower organization of collagen fibers. The term annulus however (not following Francillon-Vieillot et al., 1990), refers to the low-vascularized with higher organization of collagen fibers, but usually similar in thickness as a zone. In the studied material, no clear LAGs can be observed. Instead adjacent to the annuli, numerous lines are present. To avoid nomenclature problems, all lines representing the cessation of growth are referred in this study as resting lines, without determination if they occur annually or not (Konietzko-Meier & Sander, 2013; also see discussion).

In the thin sections, the average thickness of the entire bone and of each layer was estimated, expressed as an arithmetical average from three measurements of the thickness of the entire bone/layer. The thickness of the external layer was measured three times on the distance between the border line with middle region and the bottom of valleys and three times as the distance between the border line with middle region and the top of ridges. The mathematical average was calculated from these measurements. The minimum and maximum thicknesses represent the lowest and largest measurement, respectively, for each described layer. As the borders between external cortex/middle region/internal cortex were taken the line where the clearly visible increasing of the remodeling degree of the middle region is present (the number of the erosion cavities, independent of their size, is considerably higher). For the estimation of the ratio between the three components (E – external cortex, M – middle region, I – internal cortex; E:M:I), the average thickness of the external cortex was taken as one and then proportionally the value for middle region and internal cortex were calculated. Note that the internal cortex of dermal bone is oriented to the visceral surface of the body, thus in parasphenoid, pterygoid and vomer the external cortex is then oriented ventrally.

A detailed description of each bone is presented in the Supplementary Material.

RESULTS

Microanatomy of dermal bones

Most dermal bones of the skull are flat plates. Only the premaxillae and maxillae possess a more complicated shape (Fig. 3). The premaxilla is built up of three branches: the dental shelf, the alary process (Schoch, 1999), and the vomeral process, which connects the dental shelf to the vomer (Fig. 3A). The maxilla is built up from two branches: the dorsal one with an ornamented external cortex, and the ventral branch with the dental shelf (Fig. 3B).

The dermal bones show the clear diploë structure (Fig. 4). The external cortex of the skull-roof bones created variably ornamentations build from a combination of grooves or tubercles and ridges (Tab. 1, Fig. 1), respectively visible in the cross-section as valleys and ridges (Fig. 4A). The thickness of the flat bones varies from under 1.5 to over 10 millimeters (Tab. 1), with different proportions between the particular layers. No constant relation can be observed between the thickness of the external cortex and the thickness of the entire bone, however the external cortex of the tabular and postparietal, two the most massive bones, is clearly thicker than in other bones (Tab. 1). The relatively thin squamosal 2 with an average thickness of only about three mm, developed an external cortex which takes up almost half of the bone thickness (Tab. 1). The largest part of the bone almost always consists of the middle region (which is about two times thicker as the external cortex), with the exception of squamosal 2, where the middle region is the thinnest (Tab. 1). The internal cortex is the thinnest of the three

layers and composes usually 40% to 90% of the thickness of the external cortex, with the exception of the pterygoid (Tab. 1).

General histology of dermal bones

External cortex. In all sections the external cortex consists of parallel-fibered bone, whereas in the valleys lamellar bone often occurs (Fig. 4B and C). The elongated osteocyte lacunae with branched canaliculi in the bone matrix are numerous (Fig. 5A). Vascular canals are mostly longitudinally oriented (Fig. 5A, B). The degree of vascularization varies from relatively low in the premaxilla and frontal, moderate in the maxilla and prefrontal, to highly vascularized in the jugal, postorbital, parietal, squamosal, quadratojugal, vomer and parasphenoid. In the nasal, postparietal, postfrontal, tabular and supratemporal, numerous vascular canals within the ridges are visible, which are arranged in rows parallel to the bony surface, whereas the valleys are avascular. The external cortex is dominated by simple vascular canals and primary osteons. In some bones (nasal, lacrimal, prefrontal, tabular, squamosal, vomer and parasphenoid), many secondary osteons and few erosion cavities are visible in the transition region to the middle layer (for details see the Supplementary Material).

Typical for the external cortex are distinct collagen fibers (Fig. 5C, D). In the premaxilla, maxilla, nasal, lacrimal, jugal, postorbital, postparietal, and quadratojugal, well-mineralized Sharpey's fibers can be observed which are relatively short but numerous, and sometimes packed densely in bundles. In the prefrontal, frontal, postfrontal, parietal, supratemporal, squamosal, tabular and vomer, Sharpey's fibers are rare and occur mostly in the deeper parts of the sculptural ridges (Fig. 5C). In the parasphenoid and pterygoid, Sharpey's fibers cannot be observed. In some bones (jugal, postorbital, postfronat, postparietal, tabular) thick fibers create

Interwoven Structural Fibers (ISF) (Fig. 5D). In the postparietal a structure resembles metaplastic bone constructed from longitudinally and transversely oriented structural fibers is visible (Fig. 5 D).

Growth marks are expressed in two ways. In the ridges of the lacrimal, frontal, jugal, postfrontal, tabular, quadratojugal and squamosal 2, they are manifested as a sequence of thin resting lines (Fig. 5E). In the quadratojugal, two thick annuli built up of lamellar bone alternate with two highly vascularized zones (Fig. 5F) occur.

In the postfronal, squamosal 1, supratemporal, tabular, jugal and quadratojugal, the alternations of valleys and ridges are preserved. The remains of older valleys are filled with the highly vascularized tissue which then constructed the ridges of the next generation (Fig. 5G). In the supratemporal the cementing line is visible and indicated the remodeling process is involved into the creations of a sculpture (Fig. 5H).

Middle region. The external cortex changes gradually into the cancellous middle region. The simple vascular canals and primary osteons, of various shapes, are mostly located next to the border between the middle and external regions. A significant part of the middle region is strongly remodeled. The few large erosion cavities (up to 2000 µm in diameter) are present in the premaxilla, nasal, lacrimal, jugal, prefrontal, postparietal, squamosal 1, quadratojugal and all studied bones from the palatal side of the skull. The most highly remodeled middle region occurs in the vomer, where the trabeculae are extremely reduced and erosion cavities in some areas exceed 3000 µm in length (Fig. 6A). In the lacrimal and prefrontal, erosion cavities reach up to the external cortex. The maxilla is dominated by numerous, but medium-sized erosion cavities. In the postfrontal, parietal and supratemporal, erosion cavities are small (less than 500 µm in diameter). In the postfrontal they appear sporadically, whereas are numerous in parietal and

supratemporal (Fig. 6B). The middle region in the tabular and squamosal 2 does not show the typical trabecular structure. The intensive remodeling is visible; however, the tissue is relatively compact, almost without erosion cavities (Fig. 6C). The border between the three layers is visible as the change in the tissue organization, higher organized and more primary in cortexes and secondary in the middle region.

Internal cortex. The internal cortex consists of parallel-fibered to lamellar bone. The degree of vascularization varies from very low, almost avascular, in the parietal, postfrontal, supratemporal and squamosal, low in the premaxilla, prefrontal, nasal, and postparietal, moderate in the maxilla, frontal, vomer and parasphenoid, to high in the lacrimal, jugal, postorbital and quadratojugal (Fig. 6D-F). Osteocyte lacunae, showing slightly elongated shapes, are very frequent. Growth marks are visible in form of resting lines and a sequence of zones and annuli. The amount of lines varies from four in the postfrontal and parietal, three in the postparietal, supratemporal and jugal, to two in the nasal (Fig. 6D). In the parasphenoid, well developed zones and annuli can be observed (Fig. 6G). Zones are built of thick, well vascularized layers, while annuli are represented by thinner, avascular layers. The numerous Sharpey's fibers packed in bundles are visible in the tabular and vomer.

Endochondral bones

Quadrate. The partially preserved and well-vascularized cortex consists of parallel-fibered and lamellar bone (Fig. 7A, B). The simple vascular canals occur sporadically, and secondary osteons are more common (Fig. 7A, B). The Sharpey's fibers are very short and occur only in the subsurface parts of the cortex. The elongated osteocyte lacunae are present mainly

within the lamellar bone, which outlines the osteons. They do not possess canaliculi. Growth marks cannot be observed.

The central region consists of spongiosa and is characterized by large pore spaces and irregular trabeculae (Fig. 7C), which contain clumps of calcified cartilage (see also the Supplementary Material).

Exoccipital. The cortex consists of parallel-fibered bone and is relatively well-vascularized (Fig. 7D). The simple vascular canals are few in number (Fig. 7E, F) and located only in the outermost part of the cortex. The secondary osteons are more frequent (Fig. 7D). Well-mineralized, densely packed bundles of Sharpey's fibers are common and can be seen throughout the entire cortex (Fig. 7D, E). In the exoccipital, the Sharpey´s fibers are most abundant and pronounced among all examined bones. Rounded osteocyte lacunae are numerous. Growth marks are absent.

The central region consists of an irregular network of bony trabeculae, with large pore spaces between them (Fig. 7G). In the medial parts of the bone tissue, where trabeculae are poorly developed, accumulations of calcified cartilage are quite common (Fig. 7H).

DISCUSSION

The histological variability. Witzmann (2009) investigated fragments of dermal bones from 20 taxa and concluded that for every taxon, the bone microanatomy and histology were consistent. Intraspecific variability of the histology of dermal bones was only observed in *Mastodonsaurus giganteus* and *Plagiosternum granulosum* and affects the degree of vascularization and remodeling of the bone (Witzmann, 2009).

Nevertheless, in the *Metoposaurus krasiejowensis* skull, the variability is high and can be seen in both, microanatomical and histological levels. The bones poses various thicknesses, different proportions between the layers, variations in the vascularization systems, tissue organizations, the presence and organization of Sharpey's fibers, degree of remodeling, and growth pattern (see also the Supplementary Material for the detailed description). The combination of these characters shows that almost each sectioning-plane in the skull represents a unique framework. The transition between the „histological types" is fluent. The jugal and postorbital, sectioned in the suture region, represent the same microanatomical and histological framework (Figs. 2 j and po, 3F; Tab. 1), whereas the squamosal sectioned in the frontal part of the bone (Fig. 2, sq1) and next to the otic notch (Fig. 2, sq2), shows different architecture on both microanatomical and histological levels (Figs. 3K, L). This suggests that the histological framework is not specifically bone-limited, but seems to be related to the specific area of the skull and i.e. depended on the growth of the entire skull and each bone separately, or to the local biomechanical loading on the particular part of the skull or combination of both. Fortuny et al. (2012), based on the Finite Elements Analysis, showed that the hypothetical biomechanical stress along the skull is different for each skull-morphotype and depends directly on the shape of the skull. In consequence each taxon with different skull-morphotype because of various loading in a given region might have a unique histological architecture of homologous bones.

Remodelling degree. Among the sections from the *Metoposaurus* skull, four main remodeling degrees could be observed in the middle region. The relatively lowest remodeled samples are from the postfrontal, parietal and supratemporal. A few large erosion cavities are present in the premaxilla, nasal, lacrimal, jugal, prefrontal, postparietal, squamosal, quadratojugal and all studied bones from the palatal side of the skull. The maxilla is dominated

by numerous, but medium sized erosion cavities. In the middle region of the tabular and squamosal 2, the bone deposition exceeds the bone resorption and it does not represent the typical spongious structure.

The increase in remodeling degree is known as one of the developmental characters. Witzmann (2009) published the detailed histology of dermal bones from a young adult and adult *Mastodonsaurus,* and observed an increase in remodeling (expressed as an increase of the erosion cavities sizes) in the older specimen. In the *Metoposaurus*, different histological stages can be observed among different bones in one skull. The low (postfrontal, parietal and supratemporal) and highly (premaxilla, nasal, lacrimal, jugal, prefrontal, postparietal, squamosal, quadratojugal) remodeled bones seem to represent two stages of the same process, resulting in the increase in porosity of the middle region. This may indicate the sequence of the skull ossification during ontogeny, with the latest ossification of bones occurring on the central part of the skull roof. However, less remodeled samples originate from the grooves-ridges regions, whereas the other sections come from the reticulate areas. This confirms the hypothesis presented first by Bystrow (1935) that the polygonal reticulate structures are the center of ossification and ridges-grooves areas show the direction and extent of growth from these ossification centers. In this case, different remodeling degrees, which resemble the ontogenetic change, are the result of longitudinal growth of the bone.

Origin and dynamic of the sculpture pattern. Although dermal sculpture was early recognized as a characteristic for basal tetrapods (e.g. von Meyer, 1858; Fraas, 1889; Fritsch, 1889; Zittel, 1911), the morphogenesis of the sculptures is still questionable (summarized by Witzmann, 2009; Witzmann et al., 2010; de Buffrénil et al., 2016). Among extant tetrapods, growth of dermal bony tubercles and ridges has been studied in osteoderms of squamates and in

dermal skull bones and osteoderms of crocodiles. In squamates, the presence of pits and ridges on the external surface of osteoderms follows from both local resorption and growth of bone (Zylberberg and Castanet, 1985; Levrat-Calviac & Zylberberg, 1986), whereas in crocodile dermal bones, de Buffrénil (1982) and Cerda et al. (2015) stated that sculpture is mainly the result of local resorption. In contrast, Vickaryous and Hall (2008) found no evidence for morphogenesis of bone sculpture by resorption in *Alligator mississippiensis* and presumed that sculptural ridges develop by preferential bone growth. Concerning basal tetrapods, Bystrow (1935, 1947) showed that the development of bone sculpture in the temnospondyls *Benthosuchus*, *Platyoposaurus* and *Dvinosaurus* took place solely by growth of the bony ridges and tubercles, and resorptive processes were not involved. The thin sections of the dermal bones of skull and pectoral girdle in the basal tetrapods investigated by Witzmann (2009), corroborate Bystrow's findings and show that the dermal sculpture did not develop by local resorption of the bone surface, comparable to the pattern in basal tetrapod osteoderms (Witzmann & Soler-Gijón, 2008). According to the last study (de Buffrénil et al., 2016) the involvement of several complex remodeling processes, with the local succession of resorption and reconstruction cycles, is frequent and occurs in all major gnathostome clades, whereas the temnospondyl sections share an important common feature: the lack of superficial remodeling (resorption and reconstruction cycles). However, in the section of *Plagiosternum* describer by Witzmann (2009) the eroded external surface is illustrated. The supratemporal of *Metoposaurus krasiejowensis* (Fig. 5H) confirms the observation of Witzmann (2009) and shows that the remodeling process might be involved in the sculpture creation of Temnospondyli.

Moreover, the study of de Buffrénil et al. (2016) showed that, beside the resorption, also other dynamics processes modify the sculpture during bone growth. Buffrénil et al. (2016)

observed six main patterns of such modification. The simplest one is repetition of the width or position of pits and ridges from one growth stage to the following one. The ridges during the bone deposition can drift symmetrically in two opposite directions or the ridges around a given pit may migrate in the same direction. Also the change of size of the ridges is possible resulting in the gradual narrowing of pit diameter (convergent ridge drift) or opposite process may occur when the reduction of ridge width is observed. In most drastic case the pits can be entirely filled, and disappear to be replaced in situ by ridges.

In the skull bones of *Metoposaurus krasiejowensis* most often the new deposited bone repeats the pattern of sculptures present in the younger stages (Fig. 5D-F). However, in the postfrontal, squamosal, supratemporal, tabular, jugal, and quadratojugal the alternation of valleys and ridges is preserved (Fig. 5G). In this case the new deposited ridges are created on the place of valleys, but without resorption involved. The distance between newly created tops of the ridges is not distinctively different than of the previous generation.

It indicates that the metric pattern of the sculpture is relatively stable, but the position of the ridges and grooves is dynamic during growth as a specific adaptation to different biomechanical loading on the new, larger bone.

Skeletochronological information. Long bones generally provide the best information for bone skeletochronological studies (Castanet et al., 1993; Chinsamy-Turan, 2005; Erickson, 2005). It applies also for temnospondyls (Damiani, 2000; Steyer et al., 2004; Ray et al., 2009; Mukherjee et al., 2010; Sanchez et al., 2010a; 2010b; Konietzko-Meier & Klein, 2013; Konietzko-Meier & Sander, 2013; Konietzko-Meier & Schmitt, 2013; Sanchez & Schoch, 2013; Konietzko-Meier et al., 2014). In the long bones the three main types of growth marks is known: fast growing zones, slower deposited annuli and the Lines of Arrested Growth (LAG-s) indicated

the cessation of the growth (Francillon-Vieillot et al., 1990). Most often the full annual growth cycle consists of a thick, fast growing zone, a thin, slow growing annulus, and LAG. Moreover, in fast-growing amniotes, the several growth lines (LAG-s) present next to the surface of bone, known as the External Fundamental System (EFS) could be visible. EFS indicate a slowing down of growth, suggesting that the maximum size has been reached (Sander, 2000; Chinsamy-Turan, 2005; Erickson, 2005; Turvey et al., 2005; Sander et al., 2011). The dermal bones, e.g., osteoderms, have been used as well for skeletochronological analysis (Buffrénil & Buffetaut, 1981; Hutton, 1986; Hua & Buffrénil, 1996; Tucker, 1997; Scheyer & Sander, 2004; Hill & Lucas, 2006; Hayashi & Carpenter, 2007; Scheyer, 2007; Scheyer & Sánchez-Villagra, 2007; Hayashi et al., 2009; Klein et al., 2009). However, the results of these studies suggest a careful use of osteoderms in skeletochronology of fossil specimens because of different growth patterns between the skeleton and osteoderms (Hayashi et al., 2009; Klein et al., 2009).

Even less is known about the preservation of growth marks in the temnospondyl dermal bones. The numerous growth marks present in the external and internal cortices of the dermal bone, have been observed in several temnospondyl taxa (Scheyer, 2007; Witzmann, 2009). However, without testing the whole growth series, it is not possible to estimate the amount of remodeled tissue and thus, no direct conclusion about the individual age of sectioned bones can be provided.

Metoposaurus krasiejowensis is well known about the histology of the long bones (Konietzko-Meier & Klein, 2013; Konietzko-Meier & Sander, 2013) and the evaluation of the growth pattern preserved in long bones and dermal bones is possible. The indirect estimation of the individual age of the studied skull is possible based on the morphological characters and size-comparison with the femora. Cranial sutures were not visible on the skull surface (Gruntmejer,

2012). The disappearance of all traces of sutures on the skull surface during ontogeny is a phenomenon often encountered in adult individuals (Moazen et al., 2008). In the completely preserved skeletons of *Dutuitosaurus ouazzoui* (Dutuit, 1976), a skull of similar length (about 400 mm) as the here described, corresponds with about 142 mm long femur (Dutuit, 1976: pl XXXI; personal observation DKM). Steyer et al. (2004) calculated the individual age of the adult *Dutuitosaurus* femur, comparable in length, for eight to nine years. Comparing skeletochronological data of *Metoposaurus* with that of *Dutuitosaurus* revealed that the femora of overlapping sizes show a similar age in both taxa and strong developmental plasticity can be excluded (Konietzko-Meier & Klein, 2013). The individual age of the Krasiejów skull, based on the comparison with *Dutuitosaurus,* can be thus estimated at about eight to ten years.

In the the *Metoposaurus* skull, two types of growth alternation can be observed: in external cortex numerous resting lines in the lacrimal, frontal, jugal, postfrontal, postparietal, tabular, and quadratojugal, and alternation of thick zones and annuli in external cortex of quadratojugal (Fig. 5F) and in the internal cortex of parasphenoid (Fig. 6G). In *Metoposaurus* long bones, such aggregations of resting lines are present not only in outer part of the cortex but also deeper. It suggests that accumulation of external resting lines does not mean the cessation of growth at all (EFS), but only the oscillation in growth rate during one season (Konietzko-Meier & Klein, 2013; Konietzko-Meier & Sander, 2013). The complex with accumulation of resting lines is interpreted as the one annulus deposited during one, dry season (Konietzko-Meier & Sander, 2013; Konietzko-Meier & Klein, 2013) and together with higher vascularized zone constitutes full annual growth cycle. However, in skull the resting lines occur only once in the outermost part of external cortex following the high vascularized layer. Without the growth series it is not possible to state if the pattern known from long bones applies also for dermal

bones and older cycles have been already remodeled or dermal bones show the independent growth outline. More informative are only structures of the external cortex of quadratojugal (Fig. 5F) and internal cortex in the parasphenoid (Fig. 6G) which resembles the growth sequence seen in the *Metoposaurus* long bones (Konietzko-Meier & Klein, 2013; Konietzko-Meier & Sander, 2013). The two thick avascular layers represent the annuli, and combined with the two high vascularized zones indicate two growth seasons. Assuming that the the age of the skull is about eight/nine years, with the preservation of two growth cycles, the amount of remodeled growth marks could reach up to six to seven. This indicates a relatively fast remodeling rate of the dermal bones of the skull compared to the long bones and confirms that the dermal bones are not a good source of skeletochronological information.

Ossification processes of the skull. Quadrate bone and exoccipital show the periosteal ossification modus throughout the cartilage precursor. They consist of a trabecular middle region, surrounded by a thin layer of well-vascularized cortex. The preservation of cartilage (Fig. 7H), even during adulthood, indicates that ossification follows a pattern known for stereospondyl intercentra with relatively slow ossification of the trabecular part and late development of the periosteal cortex (Konietzko-Meier et al., 2013; Konietzko-Meier et al., 2014).

The non-endochondral bones (dermal bones) may be formed through intramembranous ossification (dermal) or metaplastic ossification. The intramembranous ossification normally occurs in the deeper layers of connective tissue of the dermis of the skin (Francillon-Vieillot et al., 1990). Metaplastic bone develops via direct transformation of pre-existing, dense connective tissue, however in the absence of a periost, osteoblasts and osteoid (Vickaryous and Hall, 2008). Most often, the metaplastic and intramembranous domains occur together creating many intermediate states between the intramebraneous bone, metaplastic bone, and even periosteal

bone (Main et al., 2005). The metaplastic component of the dermal bone represents interwoven structural fibers (Scheyer & Sander, 2004; Scheyer & Sánchez-Villagra, 2007). In *Metoposaurus* skull interwoven structural fibers are found as islets or larger areas in the external cortex in all bones from the skull roof. Moreover, in postparietal investigated here the ridges are composed completely of structural fibers. The common occurrence of ISF suggests that the metaplastic ossification plays an important role during the skull development. In contrast, the fragments of *Metoposaurus* bone described by Witzmann (2009) have an external cortex that is solely composed of well-ordered parallel-fibered bone with no metaplastic tissue. The lack of IFS may indicate that these bones sectioned by Gross (1934) do not belong to skull.

Sharpey's fibers. In the long bones of *Metoposaurus* the long Sharpey's fibers (SF1) indicate the remains of tendon and the shorter, very dense and evenly distributed fibers (SF2) are probably remains of bundles of collagenous fibers connecting periosteum to bone (Konietzko-Meier and Sander, 2013). In skull bones also both types of fibers could be recognized. In the prefrontal, frontal, postfrontal, parietal, supratemporal, squamosal, tabular and vomer, Sharpey's fibers are rare and occur mostly in the deeper parts of the sculptural ridges (Fig. 5C). In the premaxilla, maxilla, nasal, lacrimal, jugal, postorbital, postparietal, and quadratojugal, well-mineralized Sharpey's fibers are relatively short but numerous, and sometimes packed densely in bundles. This type of fibers in skull might represent the remains of tight anchorage of the dermis to the external bone surface, particularly to the sculptural ridges and tubercles, which served as the main points of anchorage for the skin.

The numerous long Sharpey's fibers packed in thick bundles are visible in the tabular. In this bone the fibers occur also in the internal cortex. In the exoccipital, Sharpey's fibers are densely packed in bundles and they are much thicker and longer (Fig. 7D) than in the other bones. The

Sharpey's fibers occur here in similar amounts to those described in vertebrae (Konietzko-Meier et al., 2013). Large concentrations of long, well mineralized Sharpey's fibers in the tabular and exoccipital seem to be the obvious remains of strong muscle attachments and ligaments which connects the skull to the vertebral column.

Summary

Among the bone of the *Metoposaurus krasiejowensis* skull, the variability is very high and can be seen in both, microanatomical and histological levels. The histological types are not specifically bone-limited, but seem to be related to the specific area of the skull. The observed pattern of remodeling progression suggest that the polygonal reticulate structures are the center of ossification and ridges-grooves areas show the direction and extent of growth from these ossification centers. The estimation of the individual age of the skull based on the morphological characters and comparison with the femora suggest the relatively fast remodeling rate of the dermal bones and confirms that the dermal bones are not a good source of skeletochronological information. The dynamic processes present in the external cortex (resorption and the alternation of the position of valleys and ridges) change the position of the ridges and grooves what is a specific adaptation to different biomechanical loading on the new, larger bone. Three main types of ossification occur in the skull. Quadrate bone and exoccipital show the periosteal ossification modus throughout the cartilage precursor. The preservation of cartilage, even during adulthood, indicates that ossification follows a pattern known for stereospondyl intercentra with relatively slow ossification of the trabecular part and late development of the periosteal cortex. The non-endochondral bones (dermal bones) may be formed through intramembranous ossification (dermal) or metaplastic ossification. The common occurrence of ISF suggests that the

metaplastic ossification plays an important role during the skull development. Short and dense Sharpey's fibers (SF2) visible in the external cortex are probably remains of tight anchorage of the dermis to the external bone surface. The numerous Sharpey's fibers packed in bundles visible in the tabular and exoccipital are the remains of strong muscle attachments and ligaments which connects the skull to the vertebral column.

ACKNOWLEDGEMENTS

The authors acknowledge Olaf Dülfer (University of Bonn, Steinman Institute) for preparing some of the thin-sections. We are grateful to Kayleigh Wiersma (University of Bonn, Steinmann Institute) for improving the English. Aurore Canoville and Martin Sander are acknowledged for fruitful discussion. We thank both reviewers (Torsten Scheyer and Ignacio Cerda) and editor (Andrew Farke) for all comments which greatly improved our paper.

REFERENCES

1. Bodzioch A, Kowal-Linka M. 2012. Unraveling the origin of the Late Triassic multitaxic bone accumulation at Krasiejow (S Poland) by diagenetic analysis. *Palaeogeography, Palaeoclimatology, Palaeoecology* 346/347:25-36.
2. Brusatte SL, Butler RJ, Sulej T, Niedźwiedzki R. 2010. The taxonomy and anatomy of rauisuchian archosaurs from the Late Triassic of Germany and Poland. *Acta Palaeontologica Polonica* 54:221-230.

3. Brusatte SL, Butler MJ, Mateus O, Steyer JS. 2015. A new species of *Metoposaurus* from the Late Triassic of Portugal and comments on the systematics and biogeography of Metoposaurid temnospondyls. *Journal of Vertebrate Paleontology* 35(3):e912988.
4. Buffrénil de V. 1982. Morphogenesis of bone ornamentation in extant and extinct crocodilians. *Zoomorphology* 99(2):155-166.
5. Buffrénil de V, Buffetaut E. 1981. Skeletal growth lines in an Eocene crocodilian skull from Wyoming as an indicator of ontogenetic age and paleoclimatic conditions. *Journal of Vertebrate Paleontology* 1:57-66.
6. Buffrénil de V, Dauphin Y, Rage JC, Sire JY. 2011. An enamellike tissue, osteodermine, on the osteoderms of a fossil anguid (Glyptosaurinae) lizard. *Comptes Rendus Palevol* 10:427-437.
7. Buffrénil de V, Clarac F, Canoville A, Laurin M. 2016. Comparative data on the differentiation and growth of bone ornamentation in gnathostomes (Chordata: Vertebrata). *Journal of Morphology* 277(5):634-70.
8. Burns M, Vickaryous MK, Currie PJ. 2013. Histological variability in fossil and recent alligatoroid osteoderms: Systematic and functional implications. *Journal of Morphology* 274:676-686.
9. Bystrow AP, 1935. Morphologische Untersuchungen der deckknochen Schädels der Stegocephalen. *Acta Zoologica* 16:65-141.
10. Bystrow AP. 1947. Hydrophilous and zenophilous labyrinthodonts. *Acta Zoologica* 28:137-164.

11. Castanet J, Francillon-Vieillot H, Meunier FJ, Ricqlès de A. 1993. Bone and individual aging. In: Hall BK [ed] Bone. Volume 7: Bone Growth–B. CRC Press, Boca Raton, Florida. 245-283.
12. Castanet J, Francillon-Vieillot H, Ricqlès de A. 2003. The skeletal histology of the Amphibia. In: Heatwole H, Davies M [eds] Amphibian Biology, Volume 5, Osteology. Surrey Beatty and Sons, Chipping Norton, New South Wales, Australia. 1598-1683.
13. Cerda IA, Desojo JB, Trotteyn MJ, Scheyer TM. 2015. Osteoderm histology of Proterochampsia and Doswelliidae (Reptilia: Archosauriformes) and their evolutionary and paleobiological implications. *Journal of Morphology* 276(4):385-402.
14. Chinsamy-Turan A. 2005. The Microstructure of Dinosaur Bone: Deciphering Biology with Fine-scale Techniques. Johns Hopkins University Press, Baltimore. 1-195.
15. Chinsamy A, Raath MA. 1992. Preparation of fossil bone for histological examination. *Palaeontologia Africana* 29:39-44.
16. Clarac F, Souter T, Cornette R, Cubo J, Buffrénil de V. 2015. A quantitative assessment of bone area increase due to ornamentation in the Crocodylia. *Journal of Morphology* 276:1183-1192.
17. Clarac F, Souter T, Cubo J, Buffrénil de V, Brochu C, Cornette R. 2016. Does skull morphology constrain bone ornamentation? A morphometric analysis in the Crocodylia. *Journal of Anatomy* doi:10.1111/joa.12470.
18. Coldiron RW. 1974. Possible functions of ornament in labyrinthodont amphibians. *Occasional Papers of the Museum of Natural History of the University of Kansas*, *Lawrence* 33:1-19.

19. Damiani RJ. 2000. Bone histology of some Australian Triassic temnospondyl amphibians: preliminary data. *Modern Geology* 24:109-124.

20. Dutuit JM. 1976. Introduction à l'etude paleontologique du Trias continental marocain. Description des premiers Stegocephales recueillis dans le couloir d'Argana (Atlas occidental). *Memoires du Museum National d'Histoire Naturelle Paris Ser. C* 36:1-253.

21. Dzik J. 2001. A new *Paleorhinus* fauna in the early Late Triassic of Poland. *Journal of Vertebrate Paleontology* 21:625-627.

22. Dzik J. 2003. A beaked herbivorous archosaur with dinosaur affinities from the early Late Triassic of Poland. *Journal of Vertebrate Paleontology* 23:556-574.

23. Dzik J. 2008. Gill structure and relationships of the Triassic cycloid crustaceans. *Journal of Morphology* 269:1501-1519.

24. Dzik J, Sulej T. 2007. A review of the early Late Triassic Krasiejów biota from Silesia, Poland. *Palaeontologia Polonica* 64:3-27.

25. Dzik J, Sulej T, Kaim A, Niedźwiedzki R. 2000. Późnotriasowe cmentarzysko kręgowców lądowych w Krasiejowie na Śląsku Opolskim. *Przegląd Geologiczny* 48:226-35.

26. Enlow DH, Brown SO. 1956. A comparative histological study of fossil and recent bone tissues. *I. Texas Journal of Science* 8:405-43.

27. Erickson GM. 2005. Assessing dinosaur growth patterns: a microscopic revolution. *Trends in Ecology and Evolution* 20(12):677-84.

28. Fortuny J, Marcé-Nogué J, de Esteban-Trivigno S, Gil L, Galobart Á. 2011. Temnospondyli bite club: ecomorphological patterns of the most diverse group of early tetrapods. *Journal of Evolutionary Biology* 24:2040-2054.

29. Fortuny J, Marce´-Nogue´ J, Gil L, Galobart Á. 2012. Skull mechanics and the evolutionary patterns of the otic notch closure in Capitosaurs (Amphibia: Temnospondyli). *The Anatomical Record* 295:1134-1146.
30. Fraas E. 1889. Die Labyrinthodonten der Schwäbischen Trias. *Palaeontographica* 36:1-158.
31. Francillon-Vieillot H, de Buffrénil V, Castanet J, Géraudie J, Meunier FJ, Sire JY, Zylberberg L, de Ricqlès A. 1990. Microstructure and mineralization of vertebrate skeletal tissues. In: Carter JG [ed.]: Skeletal Biomineralization: Patterns, Processes and Evolutionary Trends, Vol. I. Van Nostrand Reinhold, New York. 471-530.
32. Fritsch A. 1889. Fauna der Gaskohle und der Kalksteine der Permformation Böhmens, Vol. 2. Prag: Selbstverlag. 1-132.
33. Gross W. 1934. Die Typen des mikroskopischen Knochenbaues bei fossilen Stegocephalen und Reptilien. *Zeitschrift für Anatomie und Entwicklungsgeschichte* 203:731-64.
34. Gruntmejer K. 2012. Morphology and function of cranial sutures of the Triassic amphibian *Metoposaurus diagnosticus* (Temnospondyli) from southwest Poland. In: Jagt-Yazykova E, Jagt J, Bodzioch A, Konietzko-Meier D [eds] Krasiejów – palaeontological inspirations. *ZPW Plik*, Bytom. 34-54.
35. Gruszka B, Zieliński T. 2008. Evidence for a very low-energy fluvial system: a case study from the dinosaur-bearing Upper Triassic rocks of Southern Poland. *Geological Quarterly* 52:239-252.

36. Hayashi S, Carpenter K. 2007. Different growth patterns between the body skeleton and osteoderms of *Stegosaurus* (Ornithischia: Threophora). *Journal of Vertebrate Paleontology* 27 (Suppl.): 88A.

37. Hayashi S, Carpenter C, Suzuki D. 2009. Different growth patterns between the skeleton and osteoderms of *Stegosaurus* (Ornithischia, Thyreophora). *Journal of Vertebrate Paleontology* 29:123-131.

38. Hill RV, Lucas SG. 2006. New data on the anatomy and relationships of the Paleocene crocodylian Akanthosuchus langstoni. Acta Palaeontologica Polonica 51:455-464.

39. Hua S, Buffrénil de V. 1996. Bone histology as a clue in the interpretation of functional adaptations in the Thalattosuchia (Reptilia, Crocodylia). *Journal of Vertebrate Paleontology* 16:703-717.

40. Hutton JM. 1986. Age determination of living Nile crocodiles from the cortical stratification of bone. *Copeia* 2:332-341.

41. Klein N, Scheyer T, Tütken T. 2009. Skeletochronology and isotopic analysis of a captive individual of *Alligator mississippiensis* Daudin, 1802. *Fossil Record* 12(2):121-131.

42. Konietzko-Meier D, Klein N. 2013. Unique growth pattern of *Metoposaurus diagnosticus krasiejowensis* (Amphibia, Temnospondyli) from the Upper Triassic of Krasiejów, Poland. *Palaeogeography Palaeoclimatology Palaeoecology* 370:145-157.

43. Konietzko-Meier D, Sander PM. 2013. Long bone histology of *Metoposaurus diagnosticus* (Temnospondyli) from the Late Triassic of Krasiejów (Poland) and its paleobiological implications. *Journal of Vertebrate Paleontology* 35(5):1-16.

44. Konietzko-Meier D, Schmitt A. 2013. Micro-CT-scan as a new, non-invasive method for palaeohistological studies on the basis of a *Plagiosuchus* (Amphibia, Temnospondyli, Plagiosauridae) femur. *The Netherlands Journal of Geosciences* 92(2/3):97-108.

45. Konietzko-Meier D, Bodzioch A, Sander PM. 2013. Histological characteristics of the vertebral intercentra of *Metoposaurus diagnosticus* (Temnospondyli) from the Upper Triassic of Krasiejów (Upper Silesia, Poland). *Earth and Environmental Science Transactions of the Royal Society of Edinburgh* 103:1-14.

46. Konietzko-Meier D, Danto M, Gądek K. 2014. The microstructural variability of the intercentra among temnospondyl amphibians. *Biological Journal of the Linnean Society* 112:747-764.

47. Levrat-Calviac V, Zylberberg L. 1986. The structure of the osteoderms in the gekko: *Tarentola mauritanica*. *American Journal of Anatomy* 176:437-446.

48. Lucas SG. 2015. Age and correlation of Late Triassic tetrapods from southern Poland. *Annales Societatis Geologorum Poloniae* 85(4):627-635.

49. Lucas SG, Spielmann JA, Hunt AP. 2007. Bio-chronological significance of Late Triassic tetrapods from Krasiejów, Poland. *New Mexico Museum of Natural History and Science Bulletin* 41:248-258.

50. Main RP, Ricqlès de A, Horner JR, Padian K. 2005. The evolution and function of thyreophoran dinosaur scutes: implications for plate function in stegosaurs. *Paleobiology* 31:291-314.

51. Meyer H von. 1842. Labyrinthodonten—Genera. *Neues Jahrbuch für Mineralogie, Geographie, Geologie, Palaeontologie* 1842:301-304.

52. Meyer H von. 1858. Reptilien aus der Steinkohlenformation in Deutschland. *Palaeontographica* 6:59-219.

53. Moazen M, Curtis N, Evans SE, O'Higgins P, Fagan MJ. 2008. Rigid-body analysis of a lizard skull: Modelling the skull of *Uromastyx hardwickii*. *Journal Biomechanics* 41:1274-1280.

54. Mukherjee D, Ray S, Sengupta DP. 2010. Preliminary observations of the bone microstructure, growth patterns, and life habits of some Triassic Temnospondyls from India. *Journal of Vertebrate Paleontology* 30(1):78-93.

55. Olempska E. 2004. Late Triassic spinicaudatan crustaceans from southwestern Poland. *Acta Palaeontologica Polonica* 49(3):429-442.

56. Olempska E. 2011. Fresh-water ostracods from the Late Triassic of Poland. *Joannea Geologie und Paläontologie* 11:154-155.

57. Racki G, Szulc J. 2014. Formacja grabowska – podstawowa jednostka litostratygraficzna kajpru Górnego Śląska. *Przegląd Geologiczny* 63(2):103-113.

58. Ray S, Mukherjee D, Bandyopadhyay S. 2009. Growth patterns of fossil vertebrates as deduced from bone microstructure: case studies from India. *Journal of Biosciences* 34:661-672.

59. Ricqlès de A. 1981. Recherches paléohistologiques sur les os longs des tétrapodes. VI.- Stégocéphales. *Annales de Paléontologie* 67:141-160.

60. Rinehart LF, Lucas SG. 2013. The functional morphology of dermal bone ornamentation in temnospondyl amphibian. In: Tanner LH, Spielmann JA, Lucas SG [eds] The Triassic System. *New Mexico Museum of Natural History and Science, Bulletin* 61:524-532.

61. Sanchez S., Ricqlès de A, Schoch RR, Steyer JS. 2010a. Developmental plasticity of limb bone microstructural organization in *Apateon*: histological evidence of paedomorphic conditions in branchiosaurs. *Evolution & Development* 12:315-328.

62. Sanchez S, Schoch RR, Ricqlès de A, Steyer JS. 2010b. Palaeoecological and palaeoenvironmental influences revealed by longbone palaeohistology: the example of the Permian branchiosaurid *Apateon*. In : Vecoli M, Meyer CG [eds] The Terrestrialization Process: Modeling Complex Interactions at the Biosphere-Geosphere Interface. The Geological Society, London. 139-149.

63. Sanchez S, Schoch RR. 2013. Bone histology reveals a high environmental and metabolic plasticity as a successful evolutionary strategy in a long-lived homeostatic Triassic Temnospondyl. *Evolutionary biology* 40(4):627-647.

64. Sander PM. 2000. Long bone histology of the Tendaguru sauropods: implications for growth and biology. *Paleobiology* 26:466-488.

65. Sander PM, Klein N, Stein K, Wings O. 2011. Sauropod bone histology and its implications for sauropod biology. In: Klein N, Remes K, Gee CT, Sander PM [eds] Biology of the Sauropod Dinosaurs: Understanding the Life of Giants. Life of the Past (series ed. J. Farlow). Indiana University Press, Bloomington. 276-302.

66. Scheyer TM. 2007. Skeletal histology of the dermal armor of Placodontia: the occurrence of 'postcranial fibro-cartilaginous bone' and its developmental implications. *Journal of Anatomy* 211:737-753.

67. Scheyer TM, Sander PM. 2004. Histology of ankylosaur osteoderms: implications for systematics and function. *Journal of Vertebrate Paleontology* 24:874-893.

68. Scheyer TM, Sánchez-Villagra MR. 2007. Carapace bone histology in the giant pleurodiran turtle *Stupendemys geographicus*: phylogeny and function. *Acta Palaeontologica Polonica* 52:137-154.

69. Scheyer TM, Desojo JB, Cerda IA. 2014. Bone histology of phytosaur, aetosaur, and other archosauriform osteoderms (Eureptilia, Archosauromorpha). *Anatomical Record* 297:240-260

70. Schoch RR. 1999. Comparative osteology of *Mastodonsaurus giganteus* (Jaeger, 1828) from the Middle Triassic (Lettenkeuper: Longobardian) of Germany (Baden-Württemberg, Bayern, Thüringen). *Stuttgarter Beiträge zur Naturkunde Serie B (Geologie und Paläontologie)* 278:1-170.

71. Schoch RR, Milner AR. 2000. Stereospondyli. *Handbuch der Palaeoherpetologie* 3B. Munich: Verlag Dr. Friedrich Pfeil 1-230.

72. Skawina A. 2013. Population dynamics and taphonomy of the Late Triassic (Carnian) freshwater bivalves from Krasiejów (Poland). Palaeogeography, Palaeoclimatology, Palaeoecology 379:68-80.

73. Skawina A, Dzik J. 2011. Umbonal musculature and relationships of the Late Triassic filibranch unionoid bivalves. *Zoological Journal of the Linnean Society* 163:863-883.

74. Skrzycki P. 2015. New species of lungfish (Sarcopterygii, Dipnoi) from the Late Triassic Krasiejów site in Poland, with remarks on the ontogeny of Triassic dipnoan tooth plates. *Journal of Vertebrate Paleontology* 35(5):e964357.

75. Steyer JS, Laurin M, Castanet J, Ricqlès de A. 2004. First histological and skeletochronological data on temnospondyl growth: palaeoecological and

palaeoclimatological implications. *Palaeogeography, Palaeoclimatology, Palaeoecology* 206:193-201.

76. Sulej T. 2002. Species discrimination of the Late Triassic temnospondyl amphibian Metoposaurus diagnosticus. *Acta Paleontologia Polonica* 47(3):535-546.
77. Sulej T. 2005. A new rauisuchian reptile (Diapsida: Archosauria) from the Late Triassic of Poland. *Journal of Vertebrate Paleontology* 25(1):78-86.
78. Sulej T. 2007. Osteology, variability, and evolution of *Metoposaurus*, a temnospondyl from the Late Triassic of Poland. *Paleontologia Polonica* 64:29-139.
79. Sulej T. 2010. The skull of an early Late Triassic aetosaur and the evolution of the stagonolepidid archosaurian reptiles. *Zoological Journal of the Linnean Society* 158:860-881.
80. Sulej T. Majer D. 2005. The temnospondyl amphibian *Cyclotosaurus* from the Upper Triassic of Poland. *Palaeontology* 48:157-170.
81. Szulc J, Racki G, Jewuła K. 2015a. Key aspects of the stratigraphy of the Upper Silesian middle Keuper, southern Poland. *Annales Societatis Geologorum Poloniae* 85(4):557-586.
82. Szulc J, Racki G, Jewuła K, Środoń J. 2015b. How many Upper Triassic bone–bearing levels are there in Upper Silesia (southern Poland)? A critical overview of stratigraphy and facies. *Annales Societatis Geologorum Poloniae* 85(4):587-626.
83. Tucker A D. 1997. Validation of skeletochronology to determine age of freshwater crocodiles (*Crocodylus johnstoni*). *Marine &Freshwater Research* 48:343-351.
84. Turvey SP, Green OR, Holdaway RN. 2005. Cortical growth marks reveal extended juvenile development in New Zealand moa. *Nature* 435:940-943.

85. Vickaryous MK, Hall BK. 2008. Development of the dermal skeleton in *Alligator mississippiensis* (Archosauria, Crocodylia) with comments on the homology of osteoderms. *Journal of Morphology* 269:398-422.

86. Vickaryous MK, Sire JY. 2009. The integumentary skeleton of tetrapods: origin, evolution, and development. *Journal of Anatomy* 214:441-464.

87. Witzmann F. 2009. Comparative histology of sculptured dermal bones in basal tetrapods, and the implications for the soft tissue dermis. *Palaeodiversity* 2:233-270.

88. Witzmann F, Soler-Gijón R. 2008. The bone histology of osteoderms in temnospondyl amphibians and in the chroniosuchian *Bystrowiella*. *Acta Zoologica* (Stockholm) 91: 96-114.

89. Witzmann F, Scholz H, Müller J, Kardjilov N. 2010. Sculpture and vascularization of dermal bones, and the implications for the physiology of basal tetrapods. *Zoological Journal of the Linnean Society* 160:302-340.

90. Zittel KA. 1911. Grundzüge der Paläontologie (Paläozoologie). II. Abteilung. Vertebrata. Verlag von R. Oldenbourg, München and Berlin. 1-589.

91. Zylberberg L, Castanet J. 1985. New data on the structure and the growth of the osteoderms in the reptile *Anguis fragilis* L. (Anguidae, Squamata). *Journal of Morphology* 186:327-342.

Fig. 1. The skull of *Metoposaurus krasiejowensis* (UOPB 01029) from the Late Triassic of Poland. **(A)** Dorsal view of skull; **(B)** Ventral view of the skull. Scale bar equals 10 cm.

Fig. 2. The sectioning planes of the *Metoposaurus krasiejowensis* skull (UOPB 01029) from the Late Triassic of Poland. **(A)** The skull roof; **(B)** The palatal side of the skull. The sectioning planes are marked by red lines. Grey color indicates preserved parts of the skull; the destroyed or sediment-covered regions are indicated by the light yellow color. Scale bar equals 10 cm. Abbreviations ex = exoccipital, f = frontal, j = jugal, l = lacrimal, m = maxilla, n = nasal, p = parietal, pf = postfrontal, pm = premaxilla, po = postorbital, pp = postparietal, prf = prefrontal, ps = parasphenoid, pt = pterygoid, q = quadrate bone, qj = quadratojugal, sq1 = squamosal 1, sq2 = squamosal 2, st = supratemporal, t = tabular, v = vomer.

Fig. 3. General microanatomy of the skull bones of *Metoposaurus krasiejowensis* (UOPB 01029) from the Late Triassic of Poland. **(A)** premaxilla; **(B)** maxilla; **(C)** nasal; **(D)** lacrimal; **(E)** prefrontal; **(F)** jugal/ postorbital; **(G)** postfrontal; **(H)** frontal; **(I)** parietal; **(J)** supratemporal; **(K)** squamosal 1; **(L)** squamosal 2; **(M)** postparietal; **(N)** tabular; **(O)** quadratojugal; **(P)** parasphenoid; **(Q)** vomer; **(R)** pterygoid; **(S)** quadrate bone; **(T)** exoccipital. Scale bar equals 10 mm. Abbreviations: ap = alary process, ds = dental shelf, vp = vomeral process.

Fig. 4. Detailed microanatomy of the skull bones of *Metoposaurus krasiejowensis (*UOPB 01029) from the Late Triassic of Poland, based on the frontal. **(A)** A valley and two ridges; **(B)** Enlargement of (A); the external and internal cortex, and trabecular middle region with

numerous and large erosion cavities are visible; image in cross-polarized light; **(C)** The same as (B), but in plane-polarized light. Dashed lines mark the approximately border between the external cortex/middle region/internal cortex. Scale bars equal 10 mm for (A), and 500 µm for (B-C). Abbreviations: EC = external cortex, ER = erosion cavities, IC = internal cortex, LB = lamellar bone, MR = middle region, PFB = parallel-fibered bone, r = rigde, v = valley.

Fig. 5. Histology of the external cortex of the skull bones of *Metoposaurus krasiejowensis* (UOPB 01029) from the Late Triassic of Poland. **(A)** Magnification of external cortex of the frontal; **(B)** Same as (A), but in cross-polarized light; **(C)** External cortex of the tabular with distinct Sharpey's fibers in the area of the sculptural ridges; **(D)** A succession of longitudinally and transversely cut ISF parts; **(E)** The resting lines (black arrows) in the cortex of squamosal 2; **(F)** Zones and annuli present in the external cortex of the quadratojugal; **(G)** Alternation of valleys and ridges in the postfrontal, note that remains of lamellar bone in the deep part of cortex are present, representing the bottom of a valley from an older generation; **(H)** The cementing lines (white arrows) visible in the superficial part of external cortex the supratemporal. Dashed lines mark the approximate border between the external cortex/middle region/internal cortex. Images (A), (E) and (H) in plane-polarized light, others in cross-polarized light. Scale bars equal for (A-E) and (H) 100 µm and for (F)-(G) 500 µm. Abbreviations: A = annulus; FLB = fibro-lamellar bone; L-ISF = longitudinally cut Interwoven Structural Fibers; OL = osteocyte lacunae, PO = primary osteons, r = ridge, SF = Sharpey's fibers, T-ISF = transversely cut Interwoven Structural Fibers, v = valley, Z = zone.

Fig. 6. The details of the histology of the middle region and internal cortex of the skull (UOPB 01029) bones of *Metoposaurus krasiejowensis* from the Late Triassic of Poland. **(A)** Large erosion cavities present in the middle region of the vomer; **(B)** Poorly remodeled, well vascularized middle region of the parietal; **(C)** Poorly vascularized fragment of the squamosal 2; **(D)** Almost avascular internal cortex with resting lines (black arrows) visible in the parietal; **(E)** Internal cortex of the premaxilla, note the relatively numerous vascular canals; **(F)** Internal cortex of the jugal with very numerous vascular, small vscular canals; **(G)** Alternation of thick annuli and zones visible in the internal cortex of the parasphenoid. Dashed lines mark the approximately border between the external cortex/middle region/internal cortex. Image (G) in cross-polarized light, others in plane-polarized light. Scale bars equal 100 μm for (D) and (G) and 500 μm for other photographs. Abbreviations: A = annulus, EC = external cortex, IC = internal cortex, MR = middle region, SO = secondary osteon, VC = vascular canals, Z = zone.

Fig. 7. Histological details of the quadrate (A-C) and exoccipital (D-H) of *Metoposaurus krasiejowensis* skull (UOPB 01029) from the Late Triassic of Poland. **(A)** Fragment of cortex of the quadrate; **(B)** The same as (A), but in cross-polarized light; **(C)** Trabecular bone of the quadrate bone; **(D)** Fragment of cortex of the exoccipital with distinct Sharpey's fibers; **(E)** Close-up of (D), note that the Sharpey's fibers are also visible in plane-polarized light; **(F)** The same as (E) but in cross-polarized light. Both images (E) and (F) are rotated clockwise for better arrangement of the figures; **(G)** Trabeculae visible in the central part of the exoccipital; **(H)** Remains of calcified cartilage preserved in the trabeculae part of exoccipital. Images (A), (C), (E), and (G) in plane-polarized light, others in cross-polarized light. Scale bars equal 500 μm for (C), (D) and (G), and 100 μm for other photographs. Abbreviations: C = cortex, CC = calcified

cartilage, ER = erosion cavities, LB = lamellar bone, OL = osteocyte lacunae, PO = primary osteons, PFL = parallel-fibered bone, SO = secondary osteons, SF = Sharpey's fibers, TR = trabecular region, VC = vascular canals.

Table 1(on next page)

Microanatomy of the sampled bones of *Metoposaurus krasiejowensis* skull (UOPB 01029).

[1]The average thickness of entire bone was estimated in thin sections, expressed as an arithmetical average from three measurements of the thickness of a bone taken on the bottom of valleys and the top of ridges; [2] For the estimation of ratio between external cortex (E), medial region (M) and internal cortex (I): E:M:I, the thickness of external cortex was taken as one and then proportionally the value for medial region and internal cortex were calculated; *Non-dermal bone.

Microanatomy of the sampled bones of *Metoposaurus krasiejowensis* skull (UOPB 01029).

bone	ornamentation	min-max thickness (µm)	average thickness (µm)[1]	E:M:I[2]	thickness of the external cortex (µm)
premaxilla -allary process (pm)	not preserved	3000 - 6000	4081.2	1:1.1:0.9	1331,0
maxilla (m) - dorsal process	not preserved	~3500-4500	~3060,0	1:1.1:0.9	~1020.0
nasal (n)	relatively high ridges (about 1000 µm)	4500-7000	4758.0	1:1.2:0.4	1830.0
lacrimal (l)	medium high (500 µm), steep ridges and wide grooves	4500-6500	5940.0	1:1.6:0.7	1800.0
prefrontal (prf)	medium high (500 µm) and steep ridges	3900-5000	4256.0	1:1.7:0.8	1150.0
jugal (j)	high ridges (about 1000 µm) and wide grooves	5000-8000	6940.0	1:1.5:0.7	1800.0
postorbital (po)	high ridges (about 1000 µm) and wide grooves	5000-8000	6940.0	1:1.5:0.7	1800.0
postfrontal (pf)	low ridges (about 300 µm) and shallow grooves	3500-5000	3960.0	1:1.7:0.6	1200.0
frontal (f)	high ridges (about 1000 µm) and wide grooves	4000-6000	5549.0	1:1.5:0.6	1790.0
parietal (p)	high ridges (about 1000 µm) and narrow pits	3100-4500	3840.0	1:1.6:0.6	1200.0
supratemporal (st)	high ridges (about 1500 µm) and wide grooves	2000-6500	4800.0	1:1.6:0.6	1500.0
squamosal 1 (sq1)	very high ridges (up to 2000 µm) and wide grooves	3000-5000	3915.0	1:1.2:0.7	1350.0
squamosal 2 (sq2)	high ridges (about 1000 µm) and wide grooves	1500-5000	2250.0	1:0.3:0.5	1250.0
postparietal	steep, high ridges	7000-10000	8670.0	1:1.9:0.5	2550.0

(pp)	(about 1500 μm) and polygonal pits				
tabular (t)	high ridges (about 1000 μm) and wide pits	7000-11000	10000.0	1:2.2:0.8	2500.0
quadratojugal (qj)	high ridges (about 1000 μm) and wide grooves	4000-6000	5610.0	1:1.7:0.6	1700.0
vomer (v)	no clear sculpture	2000-5000	2925.0	1:2.8:0.7	650.0
parasphenoid (ps)	no clear sculpture	2000-4700	4050.0	1:2:1.5	900.0
pterygoid (pt)	no clear sculpture	4500-7000	5460.0	1:5.4:2	650.0
quadrate bone (q)*	-	diameter 20000 μm			
exoccipital (ex)*	-	diameter 20000 μm			

[1]The average thickness of entire bone was estimated in thin sections, expressed as an arithmetical average from three measurements of the thickness of a bone taken on the bottom of valleys and the top of ridges; [2] For the estimation of ratio between external cortex (E), medial region (M) and internal cortex (I): E:M:I, the thickness of external cortex was taken as one and then proportionally the value for medial region and internal cortex were calculated;

*Non-dermal bone

Figure 1(on next page)

The skull of Metoposaurus krasiejowensis [i](UOPB 01029) from the Late Triassic of Poland.

(A) **Dorsal view of skull; (B)** Ventral view of the skull. Scale bar equals 10 cm.

A

B

Figure 2(on next page)

The sectioning planes of the Metoposaurus krasiejowensis[i] skull (UOPB 01029) from the Late Triassic of Poland.

(A) **The skull roof; (B)** The palatal side of the skull. [b]The sectioning planes are marked by red lines. Dark grey color indicates preserved parts of the skull; the destroyed or sediment-covered regions are indicated by the light grey color. Scale bar equals 10 cm. Abbreviations: pm = premaxilla, m = maxilla, n = nasal, l = lacrimal, prf = prefrontal, j = jugal, po = postorbital, pf = postfrontal, f = frontal, p = parietal, st = supratemporal, sq1 = squamosum 1, sq2 = squamosum 2, pp = postparietal, t = tabular, qj = quadratojugal, v = vomer, ps = parasphenoid, pt = pterygoid, q = quadrate bone, ex = exoccipital.

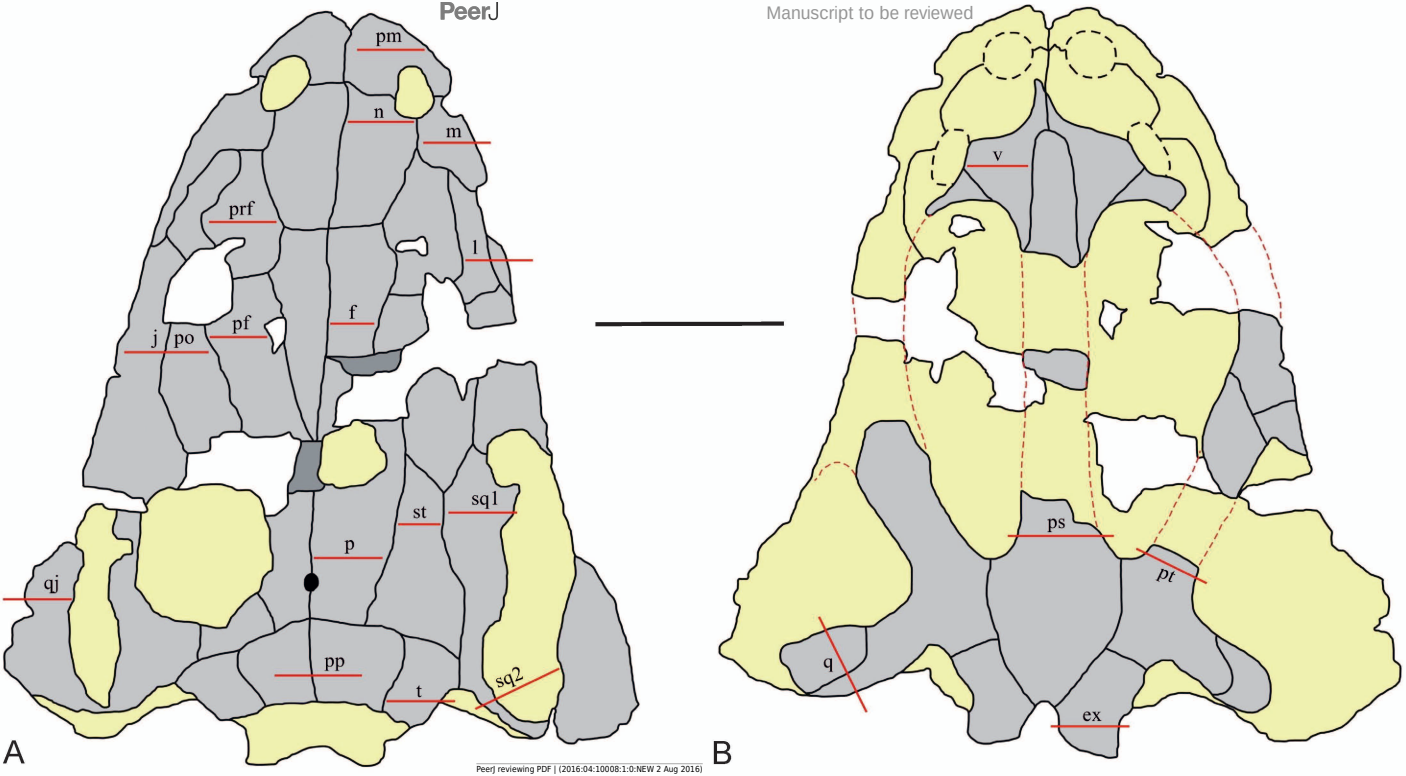
pm
n
m
prf
l
f
j
po
pf
st
sq1
p
qj
pp
t
sq2
A
v
ps
pt
q
ex
B

Figure 3(on next page)

General microanatomy of the skull bones of *Metoposaurus krasiejowensis* (UOPB 01029) from the Late Triassic of Poland.

(A) premaxilla; **(B)** maxilla; **(C)** nasal; **(D)** lacrimal; **(E)** prefrontal; **(F)** jugal/ postorbital; **(G)** postfrontal; **(H)** frontal; **(I)** parietal; **(J)** supratemporal; **(K)** squamosal 1; **(L)** squamosal 2; **(M)** postparietal; **(N)** tabular; **(O)** quadratojugal; **(P)** parasphenoid; **(Q)** vomer; **(R)** pterygoid; **(S)** quadrate bone; **(T)** exoccipital. Scale bar equals 10 mm. Abbreviations: ap = alary process, ds = dental shelf, vp = vomeral process.

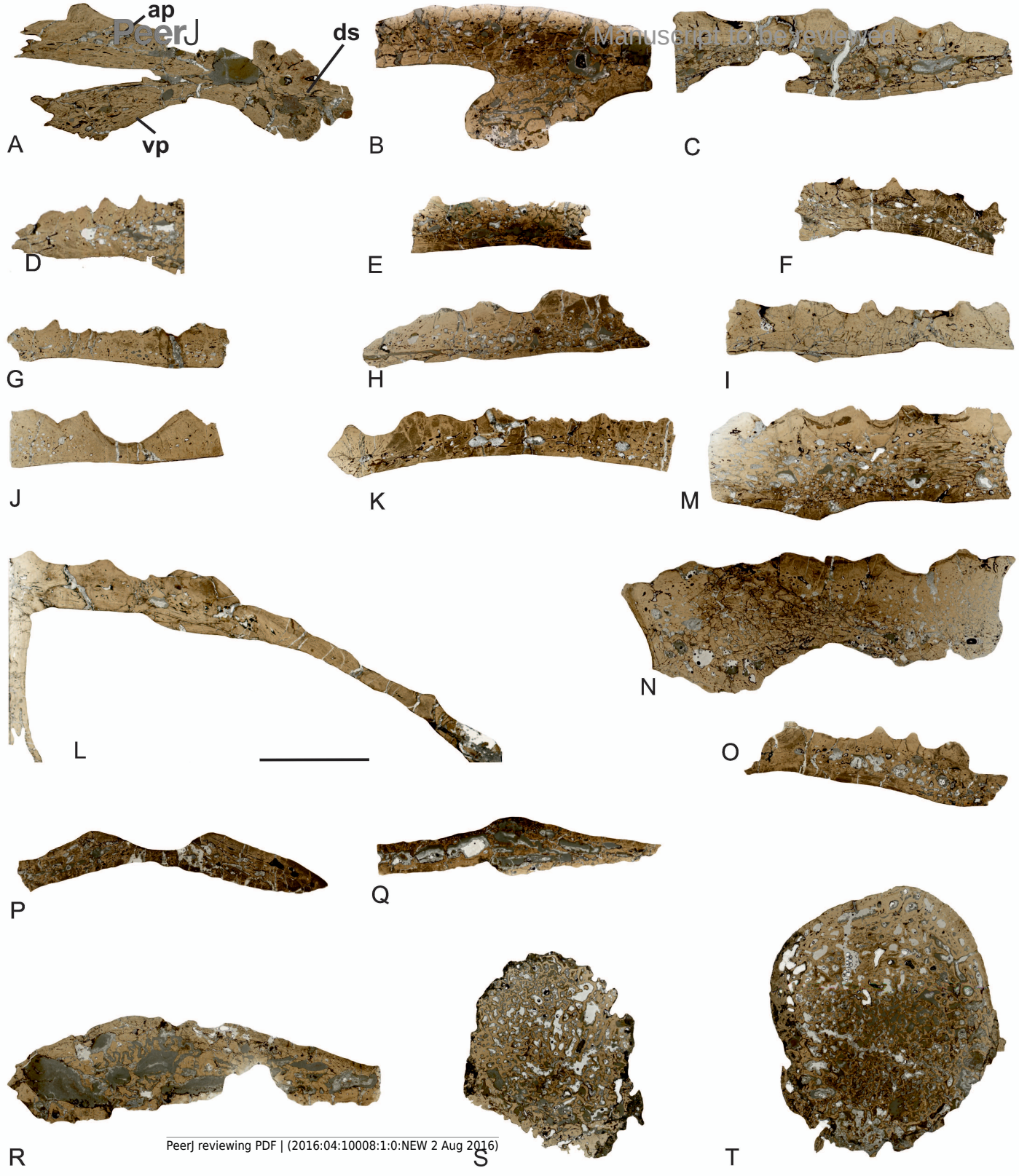

Figure 4(on next page)

Detailed microanatomy of the skull bones of *Metoposaurus krasiejowensis (*UOPB 01029) from the Late Triassic of Poland, based on the frontal.

(A) A valley and two ridges; **(B)** Enlargement of (A); the external and internal cortex, and trabecular middle region with numerous and large erosion cavities are visible; image in cross-polarized light; **(C)** The same as (B), but in plane-polarized light. Dashed lines mark the approximately border between the external cortex/middle region/internal cortex. Scale bars equal 10 mm for (A), and 500 µm for (B-C). Abbreviations: EC = external cortex, ER = erosion cavities, IC = internal cortex, LB = lamellar bone, MR = middle region, PFB = parallel-fibered bone, r = rigde, v = valley.

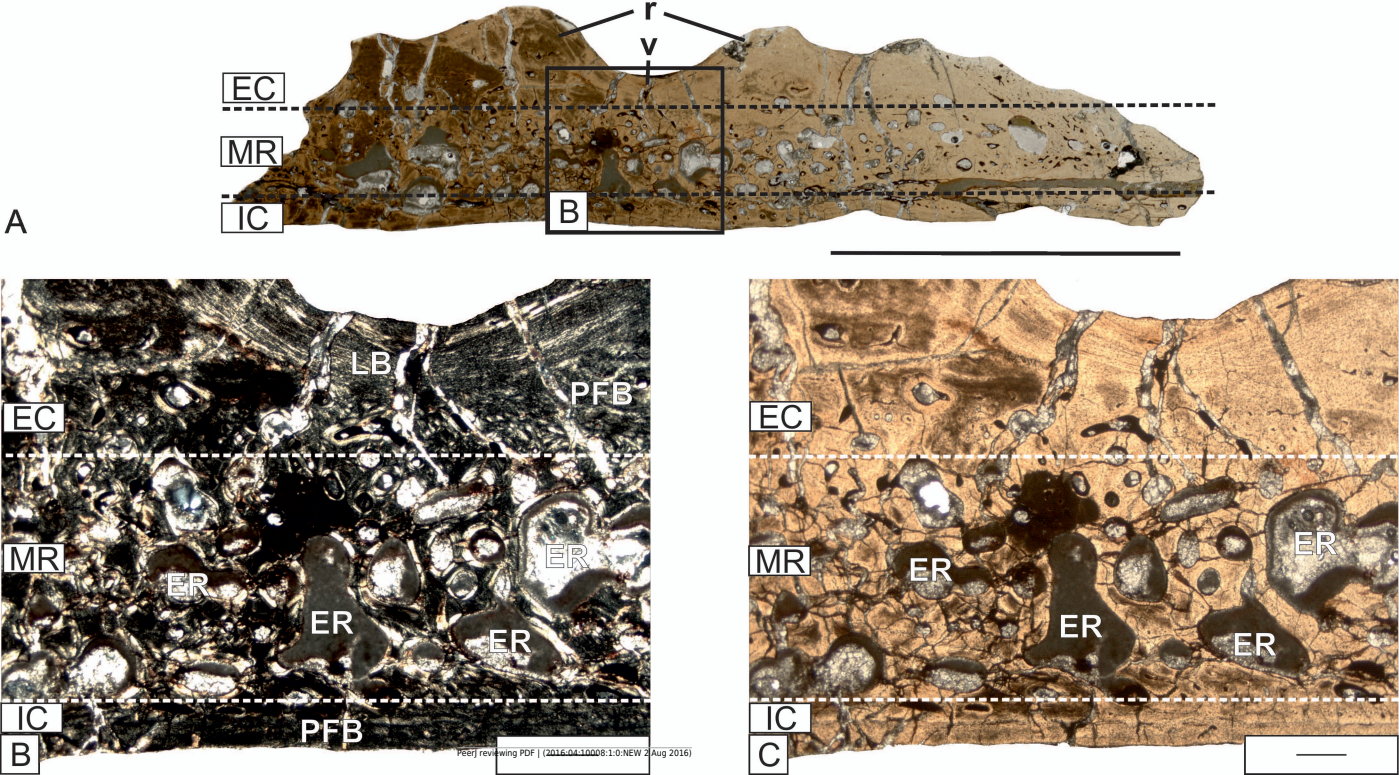
r
v
EC
MR
IC
A
B
LB
PFB
ER
C

Figure 5(on next page)

Histology of the external cortex of the skull bones of *Metoposaurus krasiejowensis* (UOPB 01029) from the Late Triassic of Poland.

(A) Magnification of external cortex of the frontal; **(B)** Same as (A), but in cross-polarized light; **(C)** External cortex of the tabular with distinct Sharpey's fibers in the area of the sculptural ridges; **(D)** A succession of longitudinally and transversely cut ISF parts; **(E)** The resting lines (black arrows) in the cortex of squamosal 2; **(F)** Zones and annuli present in the external cortex of the quadratojugal; **(G)** Alternation of valleys and ridges in the postfrontal, note that remains of lamellar bone in the deep part of cortex are present, representing the bottom of a valley from an older generation; **(H)** The cementing lines (white arrows) visible in the superficial part of external cortex the supratemporal. Dashed lines mark the approximate border between the external cortex/middle region/internal cortex. Images (A), (E) and (H) in plane-polarized light, others in cross-polarized light. Scale bars equal for (A-E) and (H) 100 µm and for (F)-(G) 500 µm. Abbreviations: A = annulus; FLB = fibro-lamellar bone; L-ISF = longitudinally cut Interwoven Structural Fibers; OL = osteocyte lacunae, PO = primary osteons, r = ridge, SF = Sharpey's fibers, T-ISF = transversely cut Interwoven Structural Fibers, v = valley, Z = zone.

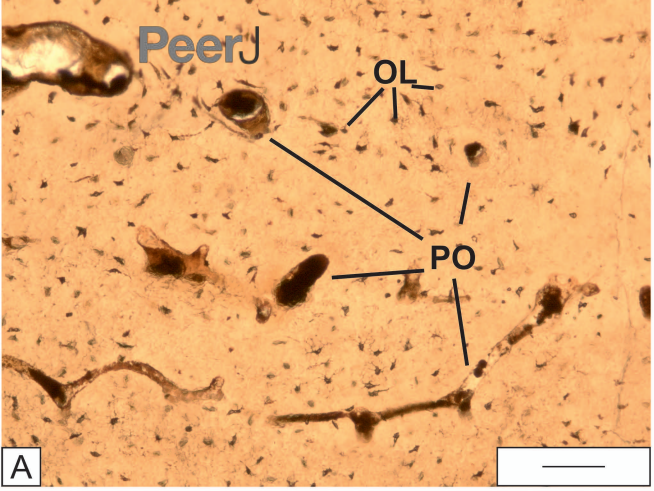

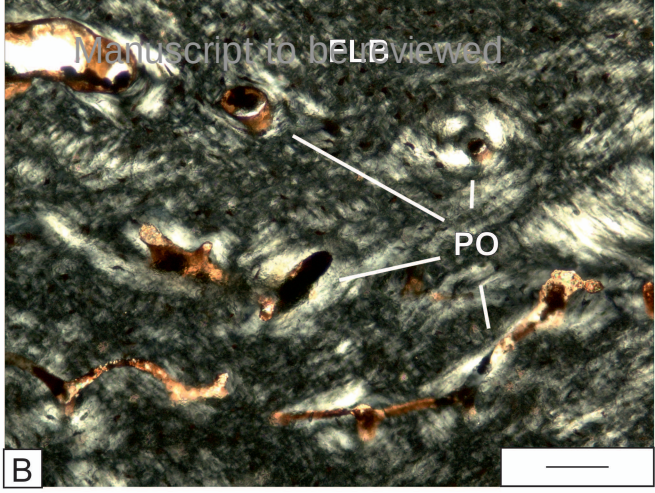

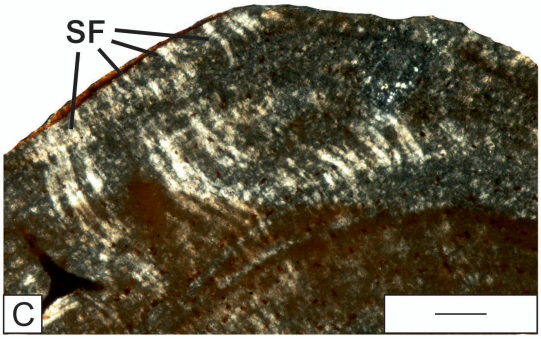

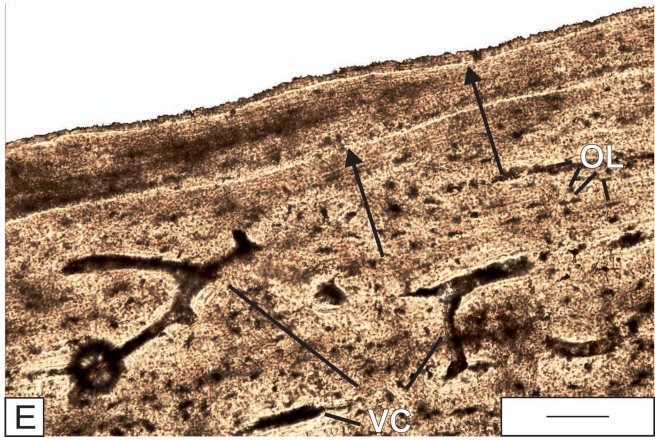

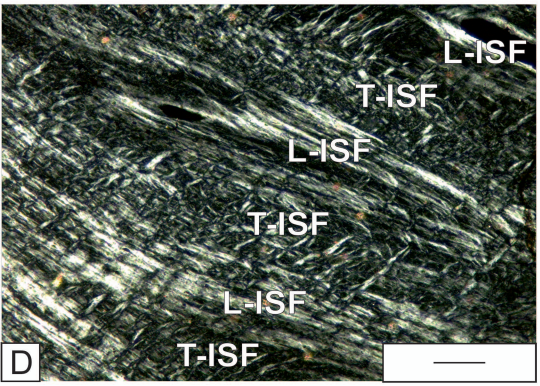

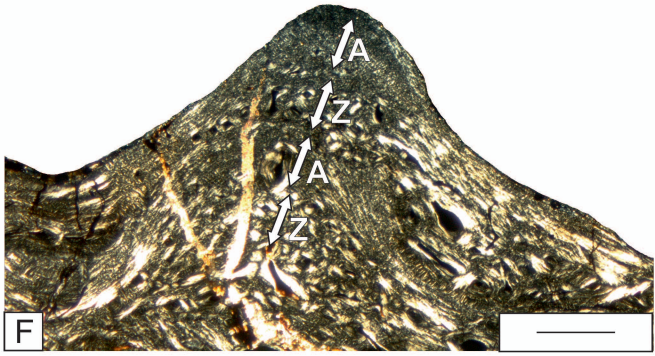

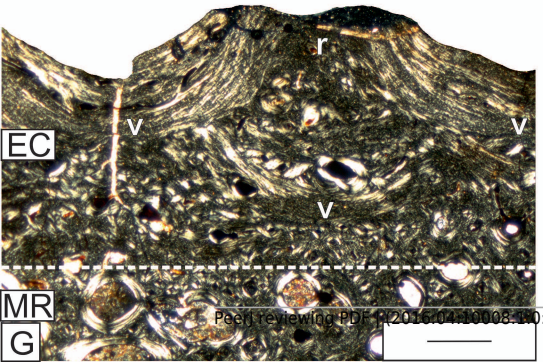

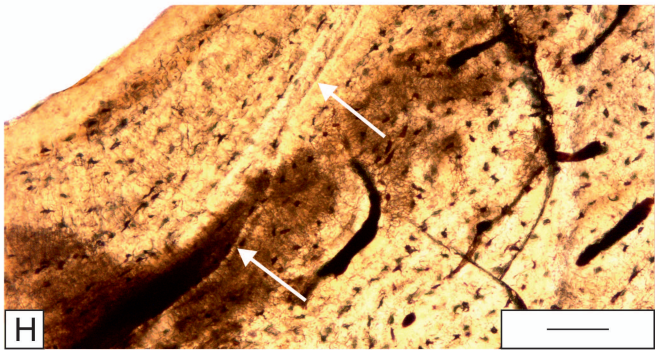

Figure 6(on next page)

The details of the histology of the middle region and internal cortex of the skull (UOPB 01029) bones of *Metoposaurus krasiejowensis* from the Late Triassic of Poland.

(A) Large erosion cavities present in the middle region of the vomer; **(B)** Poorly remodeled, well vascularized middle region of the parietal; **(C)** Poorly vascularized fragment of the squamosal 2; **(D)** Almost avascular internal cortex with resting lines (black arrows) visible in the parietal; **(E)** Internal cortex of the premaxilla, note the relatively numerous vascular canals; **(F)** Internal cortex of the jugal with very numerous vascular, small vscular canals; **(G)** Alternation of thick annuli and zones visible in the internal cortex of the parasphenoid. Dashed lines mark the approximately border between the external cortex/middle region/internal cortex. Image (G) in cross-polarized light, others in plane-polarized light. Scale bars equal 100 µm for (D) and (G) and 500 µm for other photographs. Abbreviations: A = annulus, EC = external cortex, IC = internal cortex, MR = middle region, SO = secondary osteon, VC = vascular canals, Z = zone.

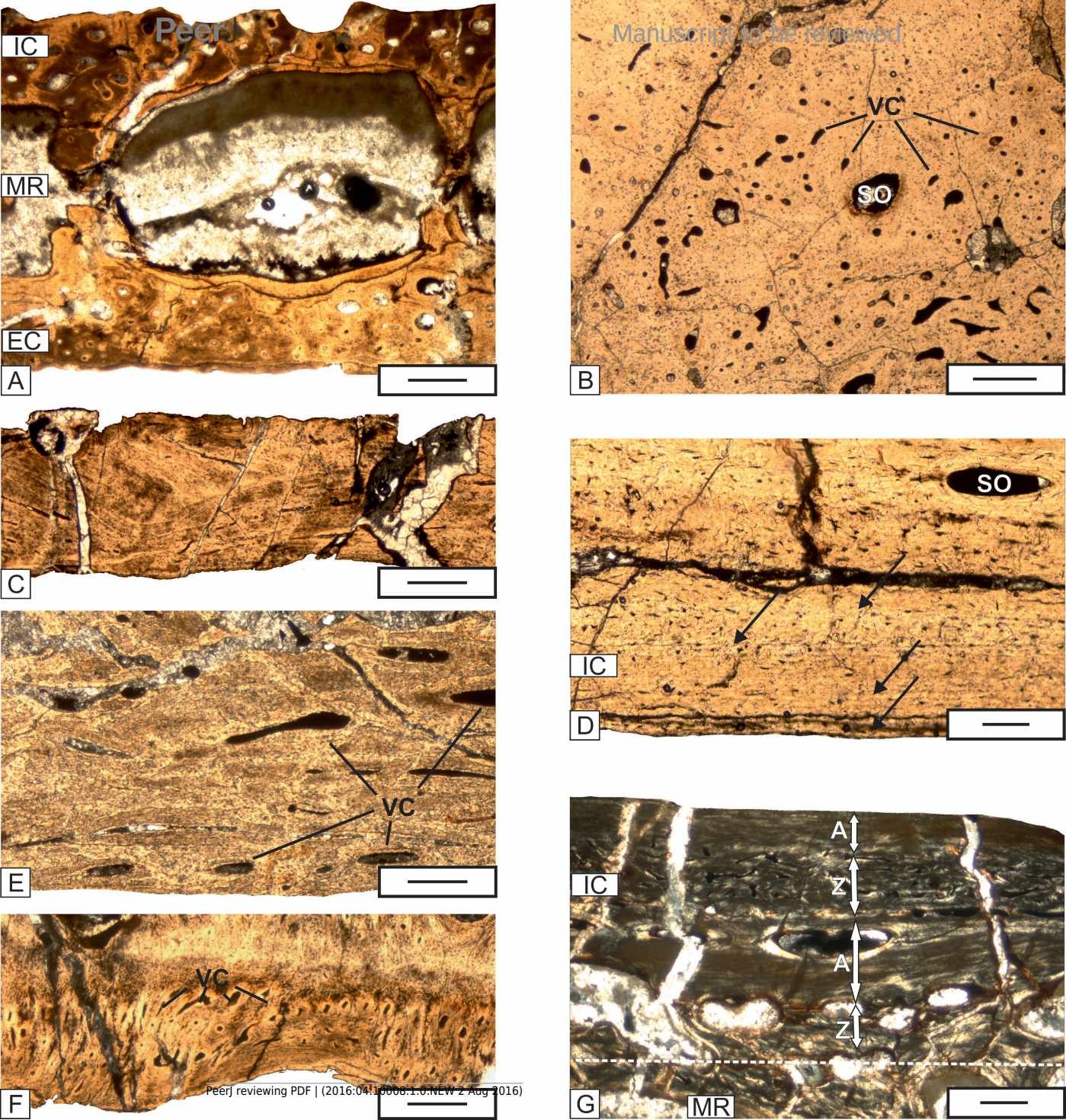

Figure 7 (on next page)

Histological details of the quadrate (A-C) and exoccipital (D-H) of *Metoposaurus krasiejowensis* skull (UOPB 01029) from the Late Triassic of Poland.

(A) Fragment of cortex of the quadrate; **(B)** The same as (A), but in cross-polarized light; **(C)** Trabecular bone of the quadrate bone; **(D)** Fragment of cortex of the exoccipital with distinct Sharpey's fibers; **(E)** Close-up of (D), note that the Sharpey's fibers are also visible in plane-polarized light; **(F)** The same as (E) but in cross-polarized light. Both images (E) and (F) are rotated clockwise for better arrangement of the figures; **(G)** Trabeculae visible in the central part of the exoccipital; **(H)** Remains of calcified cartilage preserved in the trabeculae part of exoccipital. Images (A), (C), (E), and (G) in plane-polarized light, others in cross-polarized light. Scale bars equal 500 µm for (C), (D) and (G), and 100 µm for other photographs. Abbreviations: C = cortex, CC = calcified cartilage, ER = erosion cavities, LB = lamellar bone, OL = osteocyte lacunae, PO = primary osteons, PFL = parallel-fibered bone, SO = secondary osteons, SF = Sharpey's fibers, TR = trabecular region, VC = vascular canals.